CURRENT SCIENCE AND TECHNOLOGY
e-ISSN: 2785-8804
Volume 6, Issue 1, 2026, 36 - 44
DOI: https://doi.org/10.15282/cst.v6i1.14416

RESEARCH ARTICLE

In-silico analysis of associated chitinolytic enzyme structures from aquatic bacteria

S.N. Zulkepli[1], M.S.M. Sueb[2] and S. Jamek[1]*

[1]Faculty of Industrial Sciences and Technology, Universiti Malaysia Pahang Al-Sultan Abdullah, Lebuh Persiaran Tun Khalil Yaakob, 26300 Kuantan, Pahang, Malaysia
[2]Faculty of Chemical and Process Engineering Technology, Universiti Malaysia Pahang Al-Sultan Abdullah, Lebuh Persiaran Tun Khalil Yaakob, 26300 Kuantan, Pahang, Malaysia

Abstract - Chitin is a naturally occurring polymer composed of two monomeric units and exists in three forms, namely α-, β-, and γ-chitin, which differ in their structural arrangement. Chitinolytic enzymes, known as chitinases, degrade chitin into low-molecular-weight products called chitooligomers. Extremophilic chitinases have attracted considerable interest due to their ability to function under extreme environmental conditions, making them advantageous for various industrial and biotechnological applications. In this study, an *in-silico* analysis was performed to identify putative extremophilic candidates of GH18 chitinases at various aquatic environmental adaptations, including halophilic, thermophilic, psychrophilic, and piezophilic characteristics, were considered during BLASTp screening. Five putative candidates were selected for further analysis: *Colwellia* sp. D2M02 (WP_215980056.1), *Thalassomonas viridans* (WP_084724197.1), *Bacillus thuringiensis* (WP_09832960.1), *Brevibacillus formosus* (WP_21966082.1), and *Bacillus toyonensis* (WP_098644165.1). To investigate the relationships among these candidates, analyses including primary structure characterization, multiple sequence alignment and protein domain prediction, and phylogenetic tree construction were performed. Physicochemical analyses provided insights into their chemical properties. Secondary structure prediction was carried out using RaptorX, while tertiary structure models were generated using SWISS-MODEL, RaptorX, and I-TASSER. The generated 3D models were subsequently validated using PROCHECK and Verify3D to determine the most reliable structural models. Overall, the selected putative candidates are expected to be promising for industrial-scale chitinase production due to their ability to withstand multiple extreme environmental conditions, indicating their potential as polyextremophilic enzymes.

Article History
Received : 3 April 2026
Revised : 30 June 2026
Accepted : 16 July 2026
Published : 1 September 2026

Keywords
Chitin
Chitinase
Extremophilic

1. Introduction

Chitin is a biopolymer derived from aquatic organisms. In nature, there are three polymorphic forms of chitin, namely α, β, and γ, that are differentiated by the arrangement of the polymeric chain. Chitin is a polysaccharide made up of N-acetyl-β-glucosamine that is fibrous and structured. In chitin, β (1–4) linkages connect the monomeric units of N-acetyl-d-glucosamine. Chitin is biodegraded by bacteria, insects, and plants that secrete chitinolytic enzymes. In terms of sources, it can be found in various aquatic organisms belonging of phylum Arthropoda, Porifera, Bryozoa, Molluscs, and Bacillariophyta. To date, chitin is the second most abundant biopolymer in the world next to cellulose [1]. Chitinolytic enzymes, commonly known as chitinases (E.C 3.2.2.14), are glycosyl hydrolases that cleave N-acetyl-d-glucosamine residues at the β-1,4 linkages. Exochitinases and endochitinases are the two most common types of chitinases. Exochitinases can be divided further into two subgroups based on the nature of the released product. The first is chitobiosidases (EC 3.2.1.29), which catalyse the non-reducing end of chitin microfibrils, releasing di-acetylchitobiose. The second one, 1-4-β-glucosaminidases (E.C. 3.2.1.30), involves cleaving the oligomeric products of endochitinases and chitobiosidases to generate monomers of GlcNAc. Chitinases are classified into glycosyl hydrolase families 18 and 19 based on amino acid similarity and catalytic properties. The extremophilic chitinolytic enzyme can withstand extreme conditions such as high salt concentration, high temperature, low temperature, and high pressure without denaturing the protein. This can be known as halophilic, thermophilic, psychrophilic, barophilic, and piezophilic [2]. Extremophiles are not limited to being tolerant, but they can have more than one, which can be known as a polyextremophile. They can be a great advantage for industrial applications, as they are resilient in many harsh environments and can replace enzymes modified to withstand extreme conditions. The chitinolytic enzyme has a broad range of applications that can improve human life, owing to its properties. From this, it is best for industries to use these as value-added products. Numerous industries, such as food, cosmetics, biomedical, agriculture, and waste management, have successfully utilised the chitinolytic enzyme.

Due to its abundant availability, resulting from the slow biodegradation of crustaceans' shell waste, a large accumulation has raised major concerns for the seafood processing industry. The annual natural production rate of chitin is estimated to be around 1011 tonnes worldwide [3]. In fact, improper management of these wastes can harm the environment [4]. Therefore, an eco-friendly way to utilise this material can help address issues related to industrial waste and the environment. Therefore, this study aims to identify putative candidates of extremophilic chitinase that encompass the ability to function under extreme environmental conditions, making them advantageous for various industrial and biotechnological applications.

***CORRESPONDING AUTHOR | S. Jamek** | ✉ sharizaj@umpsa.edu.my

2. Materials and Methods

2.1 Template selection and Screening of Putative Candidates

Well-studied marine chitinolytic bacteria were identified through previous journal publications. The identified bacterial strains were searched in UniProtKB to obtain reviewed protein entries and in the NCBI Protein database to retrieve protein sequences in FASTA format. These well-characterised bacterial sequences were used as template sequences for subsequent analyses. The selected templates were *Pseudoalteromonas piscicida* (Accession number: P32823) [5] and *Bacillus subtilis* (Accession number: AAC23715.1) [6]. BLASTp analysis was subsequently performed using the template sequences to screen for potential chitinase candidates in glycoside hydrolase family 18 (GH18). The search was conducted against the non-redundant protein sequence (nr) database. Putative GH18 candidates were selected based on sequence similarity ranging from 50% to 70% relative to the template sequences. Candidate sources were restricted to aquatic-related environments, including marine, freshwater, sediment, and other aquatic habitats. Additionally, the selected candidates were required to exhibit extremophilic characteristics such as psychrophilic, thermophilic, halophilic, piezophilic, or barophilic adaptations corresponding to their environmental origins. All selected putative candidates were identified as unreviewed protein entries.

2.2 Multiple Sequence Alignment

Multiple alignment of both templates (P32823 and AAC23715.1) was performed together with putative candidates using Clustal Omega for comparative purposes. The conserved motif regions of DXDXE and SXGG reported by [7] were manually examined. The ‘show colours’ option was selected to ease the examination of the motif.

2.3 Prediction of Domain

Domain prediction of the putative GH18 chitinase candidates was performed using InterPro. Upon completion of the analysis, the domains of each putative candidate were examined, with emphasis placed on InterPro entries. Information related to the identified domains was subsequently analysed.

2.4 Phylogenetic Tree Analysis

Offline software was downloaded and used, namely ‘Mega11’ (64-bit) for Windows users. To study the relationship and connection between potential candidates and the used templates: *Pseudoalteromonas piscicida* (P32823) and *Bacillus subtilis* (AAC23715.1). Protein sequence alignment was performed, and phylogenetic trees were created using the neighbour-joining method with the p-distance model and complete deletion of gaps/missing data treatment [8], [9], [10].

2.5 Physico-Chemical Analysis

The physicochemical analysis was performed using ProtParam. The parameters computed by ProtParam included molecular weight, theoretical pI, instability index, grand average of hydropathicity (GRAVY), and the total number of positively and negatively charged residues. From the five putative candidates, the best candidate was selected based on the three criteria: an instability index below 40 (where lower values indicate greater stability), the highest aliphatic index, and the lowest GRAVY value. Subsequent analyses were performed only on the selected best chitinase candidate.

2.6 Secondary and Tertiary Structure Prediction

The secondary structure, including helices and sheets, of the chitinase candidate sequences was predicted using RaptorX. This step was crucial for understanding the protein's structural features. RaptorX achieves higher accuracy in predicting protein structure and solvent accessibility in the input sequence. The proportions of α-helix, β-sheets, and coiled structures in the sequences were also included in the evaluation results [11]. For 3D structure prediction, two modelling web tools were used: I-TASSER and Swiss-Model [11], [12], [13].

2.7 Validation of the Predicted 3D Models

The 3D models generated by two modelling tools (SWISS-MODEL and I-TASSER) were then validated using the Qualitative Model Energy Analysis (QMEAN) tools. An atomic model's compatibility with its own amino acid was investigated using the Verify3D analysis tool, and a high Verify3D score indicates that the protein model is of good quality [15], [16]. The stereochemical properties of the 3D structures were checked using Ramachandran plot analysis with the PROCHECK tool. The stereochemical characteristics derived from high-resolution structures were compared with the activity of residues in the best putative GH18 chitinase candidate [17]. Lastly, the selection of the three models from three different protein structure prediction tools was done by comparing the result of PROCHECK and Verify3D.

3. Results and Discussion

3.1 Selection of Putative Candidates

Five putative chitinase candidates were identified using BLASTp searches against the databases, as shown in Table 1. These candidates were further screened based on their source habitats to assess potential extremophilic characteristics.

Table 1. The five putative chitinase candidates and their templates

Species	Identical Percentage	Accession Number
Template 1*: Pseudoalteromonas piscicida*		P32823
Colwellia sp. D2M02	65.71%	WP_215980056.1
Thalassomonas viridans	62.66%	WP_084724197.1
Template 2: *Bacillus subtilis*		AAC23715.1
Bacillus toyonensis	53.03%	WP_098644165.1
Brevibacillus formosus	61.42%	WP_21966082.1
Bacillus thuringiensis	52.75%	WP_09832960.1

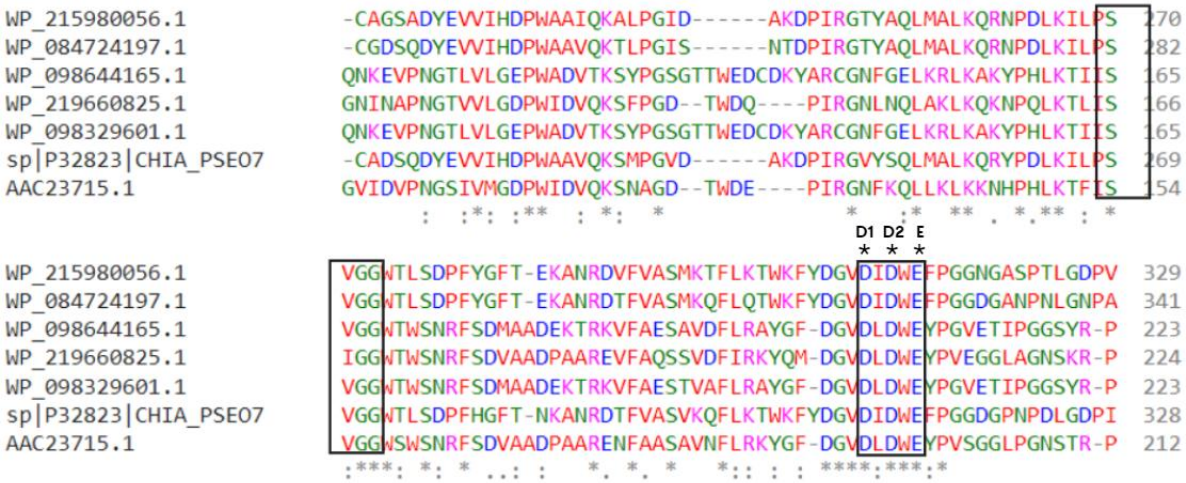

Figure 1. Sequence alignment of five putative chitinase candidates together with the templates *Pseudoalteromonas piscicida* (P32823) and *Bacillus subtilis* (AAC23715.1)

3.2 Multiple Sequence Alignment

Based on the multiple alignment analysis, all putative chitinase candidates contained the catalytic acid motif DXDXE, a conserved region of the GH18 family (Figure 1). D1 and D2, which represent Aspartate in DXDXE, are involved in hydrolytic processing [18]. D2, which is the nearest to E (Glutamate), assists in the charge stabilisation of the oxazolinium ion intermediate and the nucleophilic attack on the anomeric carbon during interaction with the N-Acetylglucosamine's (GlcNAc) N-acetyl group. Meanwhile, D1 will assist in the protonation stabilisation of D2. Glutamate (E) in DXDXE is known as the catalytic acid/base domain consensus. By contributing a proton in the first phase of the reaction, it enhances leaving group departure. After the departure, it serves as a base in the second phase of the reaction [19]. This gives the name DXDXE motif to the catalytic acid. The other motif, SXGG, where Serine (S), Glycine (G), and the X in the middle, which can be any hydrophobic amino acid, corresponds to the substrate-binding site in the GH18 family [20]. Serine in the motif is a highly conserved residue that can equally be used for the diagnostic motif. Serine will interact with the first Aspartate, D1, which is in the β-barrel relatively deep 'down' [19]. When D2 is protonated toward Glutamate, adjustment of Serine will occur with 2 consequences. Firstly, the space left by D2 will be partly filled with the adjusted side chains of Serine. Second, but perhaps more importantly, because of these changes, both residues now act as donors in strong hydrogen bonds with D1, partially compensating for the latter's negative charge.

3.3 Prediction of Domain

All putative chitinase candidates contained a Glycoside Hydrolase family 18 (GH18) catalytic domain with a conserved (β/α)8 TIM-barrel fold, consisting of eight parallel β-strands alternated with eight surrounding α-helices [21]. This domain overlaps with the glycoside hydrolase superfamily, which shares the conserved TIM-barrel catalytic framework across GH families [22], and the chitinase insertion domain (CID) superfamily, comprising five to six antiparallel β-strands and a single α-helix inserted between the seventh β-strand and α-helix of the TIM barrel. The conserved active-site motif DxxDxDxE is essential for GH18 activity, where the terminal Asp residue functions as a catalytic proton donor and stabilizes substrate distortion [21]. The CID domain further extends the substrate-binding cleft, forming a structural wall that increases cleft depth in subfamily A chitinases [23]. Additional annotations indicate functional diversity in substrate recognition. Chitinase II shows overlapping glycoside hydrolase and CID superfamily features, suggesting ligand recognition via a β-sandwich fold enriched with aromatic residues (tyrosine and tryptophan) involved in binding. Carbohydrate-binding module 2 (CBM2) belongs to subfamilies 2a and 2b, distinguished by surface-exposed tryptophan residues, and overlaps with CBM2/CBM3 and related carbohydrate-binding domain superfamilies. Fibronectin consists of repeating type I, II, and III domains and overlaps with the fibronectin type III superfamily. In chitinase A, the N-terminal region adopts a fibronectin type III–like β-strand-rich fold. Carbohydrate-binding modules 5 and 12 display a

three-stranded meander-sheet core with multiple aromatic residues important for substrate binding, consistent with their assignment to the CBM5/12 superfamily.

Figure 1. A phylogenetic tree of putative chitinase candidates with the selected chitinase templates. Both chitinase templates are selected in blue colour

3.4 Phylogenetic tree analysis

Based on the constructed phylogenetic tree shown in Figure 2, the templates and putative chitinase candidates are divided into two clades. The root of the phylogenetic tree is *Pseudoalteromonas Piscicida* (P32823), indicating that both clades share a common ancestor. The first clade is of *Bacillus subtilis* (AAC23715.1) ancestry, and the second clade is of *Thalassomonas viridans* (WP_084724197.1) ancestry. *Bacillus toyonensis* (WP_098644165.1) and *Bacillus thuringiensis* (WP_09832960.1) are sister groups since they have a common recent ancestor (located at the tips of the phylogenetic tree), namely *Bacillus subtilis* (AAC23715.1). The same goes for *Colwellia sp*. D2M02 (WP_215980056.1) and *Brevibacillus formosus* (WP_21966082.1) share the same common recent ancestor, which is *Thalassomonas viridans* (WP_084724197.1).

3.5 Physico-chemical analysis

The best putative chitinase candidate was selected based on three key parameters: instability index (protein stability in vitro), aliphatic index (indicator of thermostability), and GRAVY value (protein solubility in water). The instability index reflects protein stability, where values below 40 indicate stable proteins [24]. All candidates (shown in Table 2) were stable, with values <40, suggesting suitability for in vitro and in vivo handling. Among them, *Bacillus toyonensis* (WP_098644165.1) showed the lowest instability index (21.60), followed by *Bacillus thuringiensis* (21.76), *Thalassomonas viridans* (22.43), *Colwellia* sp. D2M02 (22.88), and *Brevibacillus formosus* (23.54). Stable proteins are often enriched in residues such as glycine, lysine, and asparagine, which contribute to structural stability. The aliphatic index (AI), defined by the relative content of isoleucine, leucine, valine, and alanine, is associated with the thermostability of globular proteins [25]. A higher AI suggests greater thermal stability. *Colwellia* sp. D2M02 exhibited the highest AI (79.02), followed by *T. viridans* (76.01), *B. formosus* (72.44), *B. thuringiensis* (68.89), and *B. toyonensis* (68.31). The relatively lower AI values in *B. toyonensis* and *B. thuringiensis* are consistent with their psychrophilic nature, as cold-adapted proteins typically show reduced thermostability [26], [27]. GRAVY values indicate protein hydrophilicity, where lower (more negative) values reflect higher solubility in water [28]. *B. toyonensis* showed the lowest GRAVY value (-0.563), followed by *B. thuringiensis* (-0.541), *B. formosus* (-0.346), *T. viridans* (-0.322), and *Colwellia* sp. D2M02 (-0.155), indicating that all candidates are generally hydrophilic, with *B. toyonensis* being the most soluble. Based on these combined criteria, *Bacillus toyonensis* (WP_098644165.1) was selected as the best candidate due to its highest stability (lowest instability index) and highest solubility (most negative GRAVY value), despite its moderate aliphatic index. Its psychrophilic nature further supports its potential functional efficiency at low temperatures, as cold-adapted enzymes typically exhibit increased structural flexibility, which enhances catalytic activity under such conditions [29].

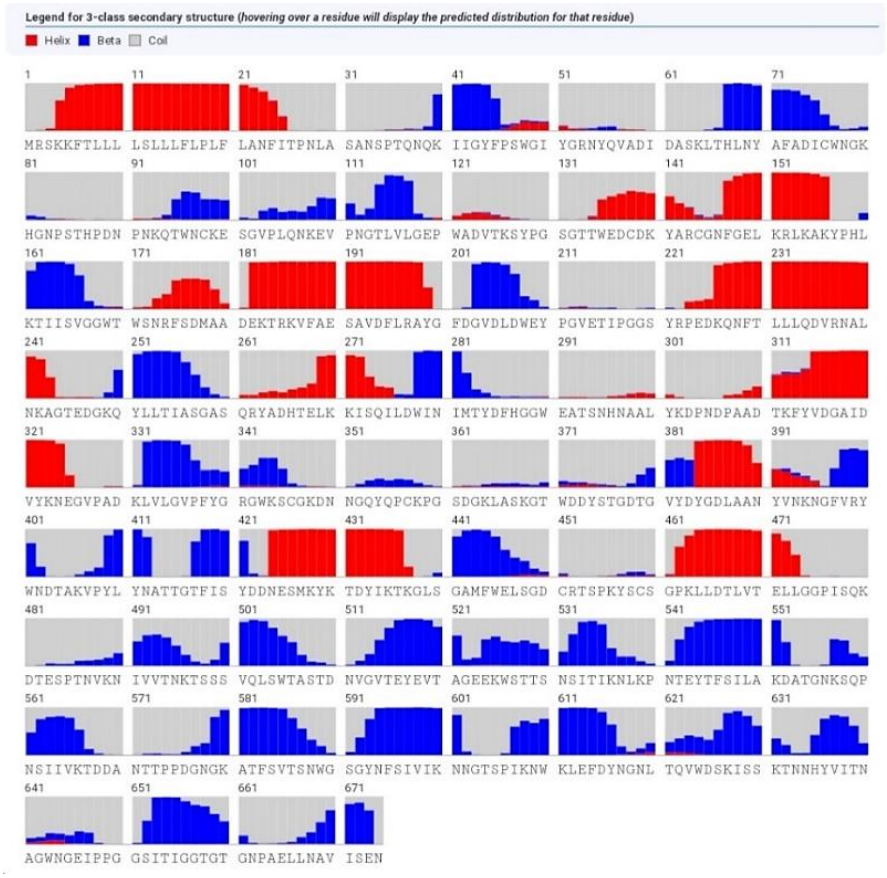

Figure 3. Three-state secondary structure prediction of *Bacillus toyonensis*

3.6 Secondary structure prediction

β-sheets and α-helices are the main structural components of proteins and their fold [30]. Based on the secondary structure prediction (Figure 3), it is shown that β-sheets are the most prevalent structure in the chitinase putative candidate *Bacillus toyonensis* (WP_098644165.1). Although it is less common than β-sheets, α-helix is also present in the structure. Proline, bends, and unstructured areas between secondary structures are common locations for certain amino acids that are likely to be found in these two structures. Similarly, amino acids like tryptophan, tyrosine, and phenylalanine, which have large ring structures in their R groups, are usually found in β-sheets. When compared to all possible combinations of alpha/beta secondary structure, the typical TIM barrel design of (β/α)8 is extremely repetitive [31].

3.7 Tertiary structure predictions

Computational methods were used to predict the 3D structure of *Bacillus toyonensis* (WP_098644165.1). SWISS-MODEL and I-TASSER were used to predict its tertiary structure. The best protein model was selected after validating the predicted 3D structures generated by these two prediction tools. Based on comparative modelling using templates, the SWISS-MODEL server was used to simulate the 3D structure of Bacillus toyonensis. Chitinase ChiA74 from *Bacillus thuringiensis* (6bt9.1) was selected as a template for model building. It has a resolution of 2.3 Å and shares 94.39% sequence identity *with Bacillus toyonensis*. The 3D models predicted using SWISS-MODEL and I-TASSER are shown in Figure 4 and Figure 5, respectively. The α-helices, β-sheets, and the coil structure cause it to take the shape of a globular protein, where it is folded into a compact structure due to hydrogen bonding and side-chain interactions.

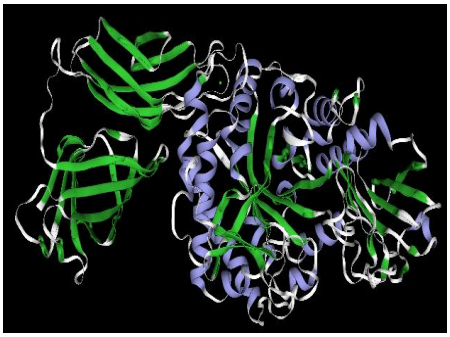

Figure 4. The 3D model of a putative GH18 chitinase candidate from *Bacillus subtilis*, namely *Bacillus toyonensis.* Respectively, the blue, green, and white colours of protein strands represent α-helix, β-sheets, and coils

Figure 5. The best model generated by I-TASSER, model 1. The fuchsia, yellow and white colours indicate α-helix, β-sheet, and coil, respectively

Table 2. Physicochemical characterization of the five putative chitinase candidate

Parameters	Putative chitinase candidates				
	Colwellia sp. D2M02 (WP_215980056.1)	*Thalassomonas viridans* (WP_084724197.1)	*Bacillus toyonensis* (WP_098644165.1)	*Brevibacillus formosus* (WP_21966082.1)	*Bacillus thuringiensis* (WP_09832960.1)
Number of amino acids	874	884	674	729	674
Molecular weight (kDa)	92.74092	95.1544	74.20453	77.99639	74.15353
Theoretical pI	4.41	4.46	5.77	4.74	5.67
Instability index	22.88	22.43	21.60	23.54	21.76
Aliphatic index (AI)	79.02	76.01	68.31	72.44	68.89
Grand average of hydropathicity (GRAVY)	-0.155	-0.322	-0.563	-0.346	-0.541
Total number of negatively charged residues (Asp + Glu)	100	113	73	71	72
Total number of positively charged residues (Arg + Lys)	51	61	66	49	64

3.8 Assessment and Validation of the Predicted 3D Model

QMEAN4 and Z-score values are the two parameters used to determine the structural validity of *Bacillus toyonensis* through QMEAN-Z score analysis. The Z-score is determined by comparing the modelled structures with template structures from the database obtained by high-resolution X-ray crystallography. The validity of modelled structures is assessed by the QMEAN4 score, which ranges from 0 to 1. Z-scores are considered acceptable if they fall within the dark zone, indicating a good model. The QMEAN Z-score of the model generated by SWISS-MODEL was in the dark zone, with a value less than 1 (Figure 6). The reported QMEAN value was 0.92, indicating that the modelled structure is valid and reliable. The local quality estimate showed residue scores ranging from 0.8 to 1.0, within the graph's range of 0.3 to 1.0, further supporting the model's reliability. In the Ramachandran plot analysis, 90.8% of the amino acid residues were in the most favoured regions, while 9.2% were in the additionally allowed regions. No residues were found in the generously allowed or disallowed regions. Therefore, 100% of the residues were located within acceptable regions, indicating that the protein structure predicted by SWISS-MODEL possesses excellent stereochemical quality. In addition, the model passed the Verify3D analysis, with 96.64% of the residues having an averaged 3D-1D score greater than or equal to 0.2.

In contrast, the Z-score of the I-TASSER model fell outside the dark zone, indicating a value greater than 2 and suggesting that the model was less acceptable (Figure 6). The reported QMEAN value was -2.84. A lower QMEAN value indicates that the model falls outside the acceptable range, suggesting lower validity and reliability. The local quality estimate for the I-TASSER model ranged from 0.2 to 1.0, with most residues scoring between 0.6 and 0.9. The Ramachandran plot analysis showed that 79.5% of amino acid residues were in the most favoured regions, 18.6% in the additionally allowed regions, 1.6% in the generously allowed regions, and 0.3% in the disallowed regions. Overall, 98.1% of the residues were located within the most favoured and additionally allowed regions, suggesting that the model possessed high stereochemical quality. Furthermore, the model passed the Verify3D analysis, with 93.18% of residues having an averaged 3D-1D score greater than or equal to 0.2.

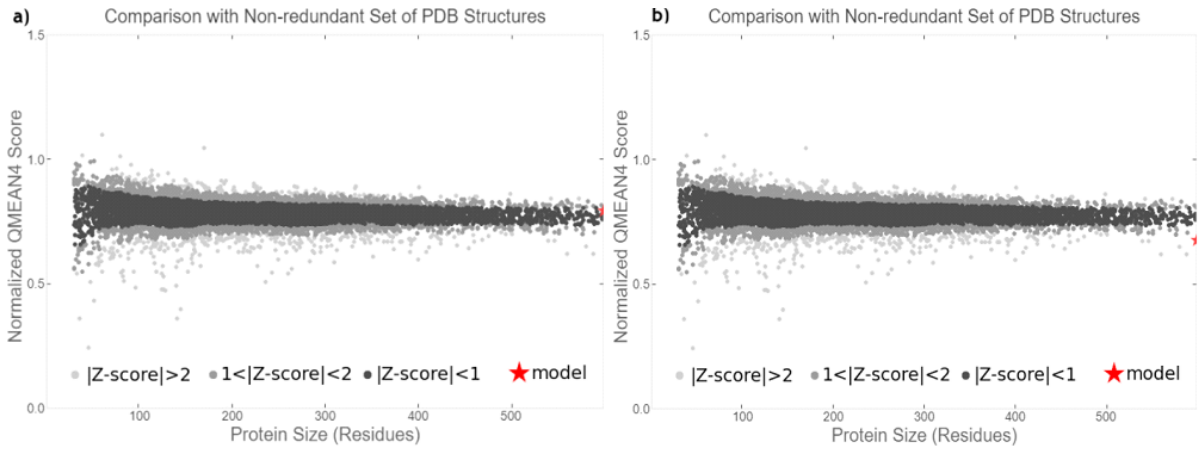

Figure 6. QMEAN score analysis of a) 3D model predicted by SWISS-MODEL a) 3D model predicted by I-TASSER

3.9 Best Model Prediction

Based on the validation analyses performed using ExPASy and SAVES Server, the 3D model generated by SWISS-MODEL was identified as the most reliable among the predicted structures. This conclusion is supported by its Z-score, which was close to 0, and its QMEAN4 value of 0.92, indicating good model quality. In contrast, the model generated by I-TASSER showed Z-scores outside the acceptable range and lower QMEAN4 values of -2.45 and -2.84, as presented in Table 3, suggesting lower reliability of the predicted structure. SWISS-MODEL also outperformed the other predicted models in validation on the SAVES Server. The validation results obtained from the SAVES analyses, including the Ramachandran Plot and VERIFY3D assessments, are presented in Table 4. More than 95% of the protein residues for all models were located within the allowed regions of the Ramachandran plot. Among the models, SWISS-MODEL showed the highest percentage, with 100% of residues located in the acceptable regions, followed by I-TASSER with 98.1%, making it the second-best model after SWISS-MODEL. In addition, an acceptable G-factor, which represents the overall quality of bond angles and covalent geometry, generally falls between -0.5 and 0, with values closer to 0 indicating better structural quality. SWISS-MODEL recorded the value closest to 0 at -0.04, indicating excellent covalent geometry. Furthermore, SWISS-MODEL achieved the highest VERIFY3D passing score at 96.64%, followed by I-TASSER at 93.18%.

Table 3. Analysis of models by QMEAN server

Software tools	Z-scores	QMEAN4
SWISS-MODEL	<1	0.92
I-TASSER	Out of range	-2.84

Table 4. Analysis of models by SAVES server

Software tools	Favourable	Additional Allowed	Generously Allowed	Disallowed	G-factor overall	Verify3D
SWISS–MODEL	90.08%	9.2%	0%	0%	-0.04	Pass
I-TASSER	79.5%	18.6%	1.6%	0.3%	-0.38	Pass

4. Conclusions

In this study, an in-silico approach was successfully applied to identify a putative GH18 chitinase candidate, *Bacillus toyonensis* (WP_098644165), which is seen as a promising chitinase candidate with potential industrial applications due to its halophilic and psychrophilic properties. Analysis of the amino acid sequence revealed the presence of two conserved GH18 chitinase motifs, DXDXE and SXGG, in which the aspartate (D) and glutamate (E) residues act as important catalytic residues of the enzyme. Secondary structure prediction of the *Bacillus toyonensis* protein indicated the presence of α-helices, β-sheets, and coil regions. This finding was further supported by tertiary structure analysis, which showed that β-sheets were more dominant than α-helices and coil structures. The predicted 3D structure demonstrated high similarity to Chitinase ChiA74 from *Bacillus thuringiensis* (6bt9.1). In addition, the model generated by SWISS-MODEL exhibited the characteristic (TIM)-barrel structure commonly found in GH18 chitinases, further supporting the reliability of the predicted model. Overall, the main objective of this study was successfully achieved by identifying and characterising a potential GH18 chitinase candidate from *Bacillus toyonensis*. The predicted enzyme may serve as a valuable chitinolytic enzyme with promising potential for various industrial applications.

Acknowledgements
We thank the Faculty of Industrial Sciences and Technology (FIST), Universiti Malaysia Pahang Al-Sultan Abdullah (UMPSA), for providing laboratory facilities, equipment, and technical support. We also appreciate the laboratory staff for their guidance and assistance.

Funding
This study was not supported by any grants from funding bodies in the public, private, or not-for-profit sectors.

Declaration of Competing Interests
The authors declare no conflicts of interest.

CRediT Author Contribution Statement
S.N. Zulkepli: Conceptualization; Methodology; Investigation; Data curation; Formal analysis; Writing –original draft; Visualisation; Project administration
M.S.M Sueb: Validation; Investigation; Writing –review & editing
S. Jamek: Supervision; Validation; Writing –review & editing; Resources; Writing –original draft; Visualisation; Project administration; Funding acquisition.

Availability of Data and Materials
The datasets generated and/or analysed during the current study are available from the corresponding author on reasonable request.

Ethics Statement
This study did not involve human participants or animal subjects. Ethical approval was therefore not required for this research.

Generative Artificial Intelligence Disclosure
The authors claim that artificially intelligent-assisted technologies, such as generative AI, were not used to generate content, ideas, or theories. We have used AI only to enhance readability and refine the language. This was used with extreme human control and oversight. The authors take full responsibility for reviewing and approving the content.

References
[1] X. Huang, J. Sun, and J. Sun, "A car-following model considering asymmetric driving behavior based on long short-term memory neural networks," *Transportation Research Part C: Emerging Technologies*, vol. 95, pp. 346–362, 2018, https://doi.org/10.1016/j.trc.2018.07.022.
[2] M. Bibra, R. N. Krishnaraj, and R. K. Sani, "An overview on extremophilic chitinases," in *Extremophilic Enzymatic Processing of Lignocellulosic Feedstocks to Bioenergy*. Cham, Switzerland: Springer, pp. 225–247, 2017, https://doi.org/10.1007/978-3-319-54684-1_12.
[3] D. Elieh-Ali-Komi and M. R. Hamblin, "Chitin and chitosan: Production and application of versatile biomedical nanomaterials," *International Journal of Advanced Research*, vol. 4, no. 3, pp. 411–427, 2016.
[4] S. N. Das, C. Neeraja, P. Sarma et al., "Microbial chitinases for chitin waste management," in *Microorganisms in Environmental Management: Microbes and Environment*. Dordrecht, Netherlands: Springer, pp. 135–150, 2012, https://doi.org/10.1007/978-94-007-2229-3_6.
[5] S. S. Paulsen, B. Andersen, L. Gram, and H. Machado, "Biological potential of chitinolytic marine bacteria," *Marine Drugs*, vol. 14, no. 12, p. 230, 2016, https://doi.org/10.3390/md14120230.
[6] S. Wang, G. Fu, J. Li et al., "High-efficiency secretion and directed evolution of chitinase BcChiA1 in *Bacillus subtilis* for the conversion of chitinaceous wastes into chitooligosaccharides," *Frontiers in Bioengineering and Biotechnology*, vol. 8, p. 432, 2020, https://doi.org/10.3389/fbioe.2020.00432.
[7] S. B. Jamek, C. Nyffenegger, J. Muschiol, J. Holck, A. S. Meyer, and J. D. Mikkelsen, "Characterization of two novel bacterial type A exo-chitobiose hydrolases having C-terminal 5/12-type carbohydrate-binding modules," *Applied Microbiology and Biotechnology*, vol. 101, no. 11, pp. 4533–4546, 2017, https://doi.org/10.1007/s00253-017-8198-4.
[8] S. Kumar, G. Stecher, M. Li, C. Knyaz, and K. Tamura, "MEGA X: Molecular Evolutionary Genetics Analysis across computing platforms," *Molecular Biology and Evolution*, vol. 35, no. 6, pp. 1547–1549, 2018, https://doi.org/10.1093/molbev/msy096.
[9] M. Nei and S. Kumar, *Molecular Evolution and Phylogenetics*. New York, NY, USA: Oxford University Press, 2000.
[10] N. Saitou and M. Nei, "The neighbor-joining method: A new method for reconstructing phylogenetic trees," *Molecular Biology and Evolution*, vol. 4, no. 4, pp. 406–425, 1987, https://doi.org/10.1093/oxfordjournals.molbev.a040454.
[11] M. Källberg, H. Wang, S. Wang et al., "Template-based protein structure modeling using the RaptorX web server," *Nature Protocols*, vol. 7, no. 8, pp. 1511–1522, 2012, https://doi.org/10.1038/nprot.2012.085.

[12] A. Waterhouse, M. Bertoni, S. Bienert et al., "SWISS-MODEL: Homology modelling of protein structures and complexes," *Nucleic Acids Research*, vol. 46, no. W1, pp. W296–W303, 2018, https://doi.org/10.1093/nar/gky427.
[13] A. Roy, A. Kucukural, and Y. Zhang, "I-TASSER: A unified platform for automated protein structure and function prediction," *Nature Protocols*, vol. 5, no. 4, pp. 725–738, 2010, https://doi.org/10.1038/nprot.2010.5.
[14] P. Benkert, M. Biasini, and T. Schwede, "Toward the estimation of the absolute quality of individual protein structure models," *Bioinformatics*, vol. 27, no. 3, pp. 343–350, 2011, https://doi.org/10.1093/bioinformatics/btq662.
[15] J. U. Bowie, R. Lüthy, and D. Eisenberg, "A method to identify protein sequences that fold into a known three-dimensional structure," *Science*, vol. 253, no. 5016, pp. 164–170, 1991. https://doi.org/10.1126/science.1853201.
[16] R. Lüthy, J. U. Bowie, and D. Eisenberg, "Assessment of protein models with three-dimensional profiles," *Nature*, vol. 356, no. 6364, pp. 83–85, 1992, https://doi.org/10.1038/356083a0.
[17] R. A. Laskowski, M. W. MacArthur, D. S. Moss, and J. M. Thornton, "PROCHECK: A program to check the stereochemical quality of protein structures," *Journal of Applied Crystallography*, vol. 26, no. 2, pp. 283–291, 1993, https://doi.org/10.1107/S0021889892009944.
[18] W. Churklam and R. Aunpad, "Enzymatic characterization and structure-function relationship of two chitinases, LmChiA and LmChiB, from *Listeria monocytogenes*," *Heliyon*, vol. 6, no. 7, p. e04252, 2020, https://doi.org/10.1016/j.heliyon.2020.e04252.
[19] G. Vaaje-Kolstad, S. J. Horn, M. Sørlie, and V. G. H. Eijsink, "The chitinolytic machinery of *Serratia marcescens*—A model system for enzymatic degradation of recalcitrant polysaccharides," *The FEBS Journal*, vol. 280, no. 13, pp. 3028–3049, 2013, https://doi.org/10.1111/febs.12181.
[20] S. M. E. Severgnini, "Isolation and characterisation of two chitinase and one novel glucanase genes for engineering plant defence against fungal pathogens," Doctoral dissertation, Murdoch University, 2006.
[21] J. Madhuprakash, A. Singh, S. Kumar et al., "Structure of chitinase D from *Serratia proteamaculans* reveals the structural basis of its dual action of hydrolysis and transglycosylation," *International Journal of Biochemistry and Molecular Biology*, vol. 4, no. 4, pp. 166–178, 2013.
[22] H. Li and L. H. Greene, "Sequence and structural analysis of the chitinase insertion domain reveals two conserved motifs involved in chitin-binding," *PLoS ONE*, vol. 5, no. 1, p. e8654, 2010, https://doi.org/10.1371/journal.pone.0008654.
[23] A. S. Lang and J. T. Beatty, "The gene transfer agent of *Rhodobacter capsulatus* and constitutive transduction in prokaryotes," *Archives of Microbiology*, vol. 175, no. 4, pp. 241–249, 2001, https://doi.org/10.1007/S002030100260.
[24] K. Guruprasad, B. V. B. Reddy, and M. W. Pandit, "Correlation between stability of a protein and its dipeptide composition: A novel approach for predicting *in vivo* stability of a protein from its primary sequence," *Protein Engineering*, vol. 4, no. 2, pp. 155–161, 1990, https://doi.org/10.1093/protein/4.2.155.
[25] E. A. Mordukhova, H. S. Lee, and J. G. Pan, "Improved thermostability and acetic acid tolerance of *Escherichia coli* via directed evolution of homoserine O-succinyltransferase," *Applied and Environmental Microbiology*, vol. 74, no. 24, pp. 7660–7668, 2008, https://doi.org/10.1128/AEM.00654-08.
[26] A. Ikai, "Thermostability and aliphatic index of globular proteins," *Journal of Biochemistry*, vol. 88, no. 6, pp. 1895–1898, 1980, https://doi.org/10.1093/oxfordjournals.jbchem.a133168.
[27] J. C. Luo, H. Long, J. Zhang, Y. Zhao, and L. Sun, "Characterization of a deep-sea *Bacillus toyonensis* isolate: Genomic and pathogenic features," *Frontiers in Cellular and Infection Microbiology*, vol. 11, p. 629116, 2021, https://doi.org/10.3389/fcimb.2021.629116.
[28] J. Hollensteiner, F. Wemheuer, R. Harting et al., "*Bacillus thuringiensis* and *Bacillus weihenstephanensis* inhibit the growth of phytopathogenic *Verticillium* species," *Frontiers in Microbiology*, vol. 7, p. 2171, 2017, https://doi.org/10.3389/fmicb.2016.02171.
[29] A. Verma, V. K. Singh, and S. Gaur, "Computational-based functional analysis of *Bacillus* phytases," *Computational Biology and Chemistry*, vol. 60, pp. 53–58, 2016, https://doi.org/10.1016/j.compbiolchem.2015.11.001.
[30] A. N. M. Ramli, N. M. Mahadi, M. S. Shamsir et al., "Structural prediction of a novel chitinase from the psychrophilic *Glaciozyma antarctica* PI12 and an analysis of its structural properties and function," *Journal of Computer-Aided Molecular Design*, vol. 26, no. 8, pp. 947–961, 2012, https://doi.org/10.1007/s10822-012-9585-7.
[31] B. Caudron and J.-L. Jestin, "Geometrical criteria for left-handed twists within protein beta-strands," *Journal of Biophysical Chemistry*, vol. 5, no. 1, pp. 5–12, 2014, https://doi.org/10.4236/jbpc.2014.51002.